JCI The Journal of Clinical Investigation

Tissue resident-like CD4+ T cells secreting IL-17 control Mycobacteria tuberculosis in the human lung

Paul Ogongo, … , Paul T. Elkington, Alasdair Leslie

J Clin Invest. 2021. https://doi.org/10.1172/JCI142014.

Research In-Press Preview **Immunology** **Infectious disease**

T cell immunity is essential for the control of tuberculosis (TB), an important disease of the lung, and is generally studied in humans using peripheral blood cells. Mounting evidence, however, indicates that tissue resident memory T cells (Trm) are superior at controlling many pathogens, including *Mycobacterium tuberculosis (Mtb)*, and can be quite different from those in circulation. Using freshly resected lung tissue, from individuals with active or previous TB, we identified distinct CD4 and CD8 Trm-like clusters within TB diseased lung tissue that were functional and enriched for IL-17 producing cells. *Mtb*-specific CD4 T cells producing TNF-α, IL-2 and IL-17 were highly expanded in the lung compared to matched blood samples, in which IL-17+ cells were largely absent. Strikingly, the frequency of *Mtb*-specific lung T cells making IL-17, but not other cytokines, inversely correlated with the plasma IL-1β levels, suggesting a potential link with disease severity. Using a human granuloma model, we showed the addition of either exogenous IL-17 or IL-2 enhanced immune control of *Mtb* and was associated with increased NO production. Taken together, these data support an important role for *Mtb*-specific Trm-like IL-17 producing cells in the immune control of *Mtb* in the human lung.

Tissue resident-like CD4+ T cells secreting IL-17 control Mycobacteria tuberculosis in the human lung.

Paul Ogongo[1,2,3,#], Liku B. Tezera[4,5,6], Amanda Ardain[1,2], Shepherd Nhamoyebonde[1,2], Duran Ramsuran[1], Alveera Singh[1], Abigail Ng'oepe[1], Farina Karim[1], Taryn Naidoo[1], Khadija Khan[1], Kaylesh J. Dullabh[7], Michael Fehlings[8], Boon Heng Lee[8], Alessandra Nardin[8], Cecilia S. Lindestam Arlehamn[9], Alessandro Sette[9,10], Samuel M. Behar[11], Adrie J. C. Steyn[1,12,13], Rajhmun Madansein[7], Henrik N. Kløverpris[1,6,14], Paul T. Elkington[4,5], and Alasdair Leslie[1, 2, 6,*]

[1]Africa Health Research Institute, Durban, South Africa. [2]School of Laboratory Medicine and Medical Sciences, University of KwaZulu-Natal, Durban, South Africa. [3]Institute of Primate Research, National Museums of Kenya, Nairobi, Kenya. [4]NIHR Biomedical Research Centre, School of Clinical and Experimental Sciences, Faculty of Medicine, University of Southampton, Southampton, UK. [5]Institute for Life Sciences, University of Southampton, Southampton, UK. [6]Department of Infection and Immunity, University College London, London, UK. [7]Department of Cardiothoracic Surgery, Nelson Mandela School of Medicine, University of KwaZulu-Natal, Durban, South Africa. [8]ImmunoScape Pte Ltd, Singapore, Singapore, [9]La Jolla Institute for Immunology, La Jolla, CA, USA. [10]Department of Medicine, University of California San Diego, La Jolla, CA 92093, USA. [11]Department of Microbiology and Physiological Systems, University of Massachusetts Medical School, Worcester, Massachusetts, USA. [12]Department of Microbiology, University of Alabama at Birmingham, Birmingham, AL 35294. [13]Centers for AIDS Research and Free Radical Biology,

University of Alabama at Birmingham, Birmingham, AL 35294. [14]Department of Immunology and Microbiology, University of Copenhagen, Copenhagen, Denmark.

[#]Present address: Division of Experimental Medicine, University of California San Francisco, San Francisco, CA, 94110, USA.

MF, BHL, and AN are shareholders and/or employees of ImmunoScape Pte Ltd. AN is a Board Director of ImmunoScape Pte Ltd.

*** Corresponding author:**

Alasdair Leslie, K-RITH tower, Nelson Mandela School of Medicine, 719 Umbilo Road, Congella, Durban, South Africa, 4001; Telephone: +27 31 2604186; e-mail: al.leslie@ahri.org

ABSTRACT

T cell immunity is essential for the control of tuberculosis (TB), an important disease of the lung, and is generally studied in humans using peripheral blood cells. Mounting evidence, however, indicates that tissue resident memory T cells (Trm) are superior at controlling many pathogens, including *Mycobacterium tuberculosis (Mtb),* and can be quite different from those in circulation. Using freshly resected lung tissue, from individuals with active or previous TB, we identified distinct CD4 and CD8 Trm-like clusters within TB diseased lung tissue that were functional and enriched for IL-17 producing cells. *Mtb*-specific CD4 T cells producing TNF-α, IL-2 and IL-17 were highly expanded in the lung compared to matched blood samples, in which IL-17+ cells were largely absent. Strikingly, the frequency of *Mtb*-specific lung T cells making IL-17, but not other cytokines, inversely correlated with the plasma IL-1β levels, suggesting a potential link with disease severity. Using a human granuloma model, we showed the addition of either exogenous IL-17 or IL-2 enhanced immune control of *Mtb* and was associated with increased NO production. Taken together, these data support an important role for *Mtb*-specific Trm-like IL-17 producing cells in the immune control of *Mtb* in the human lung.

INTRODUCTION

Tuberculosis (TB), caused by the bacterium *Mycobacterium tuberculosis* (*Mtb*), remains a leading cause of death from infectious disease worldwide (1). Despite the availability of anti-TB treatment, difficulties in diagnosis and the emergence of drug resistance warrants the need for new vaccine strategies for TB in humans (2). Approximately 25% of the global population is estimated to have been infected with *Mtb* (3), of which the majority of cases are contained by the immune system, and only 5-10% progress to active TB during their lifetime (4). The existence of protective immunity in the majority of participants gives hope that the only current vaccine in use, *Mycobacterium bovis* Bacille Calmette-Guérin (BCG), can be improved upon, as this protects infants from disseminated TB but does not provide reliable protection in adults (2).

T-cell based vaccines are promising candidates for TB (5-8), as these cells are fundamental in the prevention of primary disease after initial infection, and the development of post-primary TB after latent infection (9-11). However, the vast majority of studies seeking to identify suitable T-cell correlates of protection in human blood, which is necessary for effective vaccine design, have failed (8). One possible reason for this is that TB is primarily a disease of the lung, and parabiotic mouse experiments show that most memory T-cells in lung tissue do not recirculate in blood (12, 13). Moreover, the adoptive transfer of lung T-cells from infected mice provides better protection against *Mtb* challenge than T-cell from the blood of the same animals (14), suggesting that lung resident T-cells maybe functionally different from those in circulation.

When naïve T-cells encounter their cognate antigen they proliferate and differentiate into effector memory T-cells, which mount a rapid immune response to the same antigen following re-exposure, a process that underlies the basic principles of vaccine intervention (15-17). This memory response is often most potent at the site of infection, where a subset of non-recirculating, rapidly-responding memory T-cells, called tissue-resident memory T-cells (Trm), reside (14). Trms share functional and transcriptional similarities with central and effector memory T-cells but persist within tissues for extended periods of time, largely without recirculation back to blood (18). Because of their positioning and this rapid response time, Trm play critical roles in clearance of different infections at mucosal surfaces (19-23). This important subset is transcriptionally, phenotypically and functionally distinct from circulating T-cells (21, 24), but remains poorly characterized in humans.

Evidence for the importance of lung Trm in the response to *Mtb* comes primarily from experimental animal models, in which non-recirculating T-cells in the lung are associated with enhanced protection (25). In addition, in some, but not all cases, mucosal vaccination has been shown to offer superior protection than either subcutaneous or intradermal delivery (26-29), which has been linked to the induction of stronger Trm responses. Vaccine-specific Trms are associated with reduced bacterial loads, lung pathology and dissemination, and importantly, provide protection independently of circulating memory T-cells (28-30). However, our understanding of the lung Trm response to TB in humans is, understandably, much less complete.

To our knowledge, this study examines *Mtb*-specific lung Trms from humans for the first time. Using a unique cohort of study participants undergoing surgical lung

resections as treatment for ongoing or previous TB infection, we characterize T-cells isolated from lung tissues in comparison to matched blood from the same donor and find they express Trm markers, are highly functional, enriched for IL-17 producing subsets and are partially impaired by HIV co-infection. In addition, we find *Mtb*-specific CD4 T-cells are highly enriched in the lung, including TB-specific IL-17^{+} cells, which are largely absent from the blood. Finally, we present *ex vivo* and *in vitro* evidence that the IL-17 response is important in immune control of *Mtb* in humans.

RESULTS

TB infected human lung tissue contains functional effector memory T-cells expressing tissue-resident markers.

To examine the T-cells present in the TB infected human lung, we obtained small tissue pieces from surgically resected lungs, removed from participants with active or prior TB disease to treat their TB or post-TB sequelae. Multiple tissue sections from the same lung (typically 3) were homogenised and pooled to generate a single cell suspension and analysed by cytometry. In humans, Trms can be differentiated from circulating cells of the lung vasculature based on the expression of several surface markers associated with tissue-retention, including expression of CD69, CD103 and loss of CD62L (13, 14, 31-37). First, we applied high dimensional cytometry by time of flight (CyTOF) for detailed phenotyping of T-cell populations present in lung homogenate. Data presented in Fig.**1a** and **b** represent the cumulative staining of CD4 T-cells from 12 biological replicates, defined as having either active TB or previous TB as discussed below. T-distributed stochastic neighbour embedding analysis (TSNE)

reveals distinct clusters of T-cells within lung homogenate. As expected, given the perfused nature of lungs, this includes both $CD69^{+/-}$ CD4 T-cell populations and $CD103^{+}$ clusters express high levels CD69. The same trend is observed for CD8 T-cells (Suppl.Fig.**2a-b**). Likewise, the great majority of $CD103^{+}$ cells co-stain with ITGB7, which forms a heterodimer with CD103 to make the tissue residency integrin αEβ7, a ligand for E-cadherin. Conversely, CD62L expression is largely confined to $CD69^{-}$ clusters, as is KLRG1, a marker found to be expressed by T-cells in lung vasculature but not in the parenchyma of *Mtb* infected mice (14). Other Trm-like clusters of note include cluster 11, $CD69^{+}$ cells that co-express PD-1, TIGIT, CXCR5 and ICOS, consistent with lung resident T-follicular helper cells (38), shown to be important in the mouse model of TB (39); and cluster 16, $CD69^{+}$ cells that co-express CCR6, CCR4, classical markers of Th17 cells (40), and CD161 and CD39, novel Th17 markers (41, 42). In addition to this analysis, we grouped cells according to expression of CD69 and CD103 and tested expression levels of the other markers used. For CD4 and CD8 T-cells, 12/32 and 18/32 surface markers respectively were differentially expressed in association with CD69 and/or CD103, including upregulation of several markers associated with tissue residency in other studies such as CCR5, CCR6, CD49a, CXCR3 and CD161 (25, 43, 44) (Fig.**2**, Suppl.Fig.**1,2 and 3**).

Having shown that CD69 and CD103 positive cells in human lung express other phenotypic markers consistent with Trm, we examined the expression of these markers by flow cytometry in a larger cohort, and confirmed enrichment of CD69 and CD103 relative to the circulation and reduced expression of CD62L (Suppl.Fig.**4a and b**). Next, to investigate the impact of Mtb infection, we quantified these subsets in participants with suspected active TB or previous pulmonary TB, as determined by the

operating surgeon, based on clinical history, presentation and preoperative chest x-ray/CT scan. Macroscopically uninvolved tissue margins from participants undergoing lung cancer resection were used as non-TB controls. Microbiological confirmation was not consistently available, and therefore the treating clinician classified patients into groups at time of surgery, and clinicians were not involved in subsequent analysis. Based on this, individuals in the ATB group were enriched for $CD4^+$ and $CD8^+$ cells expressing CD69 compared to previous TB or cancer controls, reaching significance for CD8 T-cells (Fig. **3a**). The apparent bimodal distribution of CD69+ frequency was correlated to clinical characteristics, but no clear pattern was identified, although this may reflect a lack of statistical power in this group size. Similarly, the frequency of $CD103^+$ expressing CD4 and CD8 T-cells was significantly higher in the active TB group (Fig.**3b**). As reported previously, CD8 T-cells in the lung expressed higher levels of CD103 than CD4 T-cells. Approximately 50% of T-cells in lung homogenate expressed a combination of CD69 and CD103, although the relative proportions varied between participants (Suppl.Fig**.5a-c**). In contrast, expression of these markers was extremely low in matched blood samples and was not significantly different between patient groups (Suppl.Fig**.5d**). Thus, these data suggest that CD4 and CD8 Trm-like cells are present in TB diseased human lung tissue and are likely to have expanded during active TB infection.

In addition to expression of cell surface markers such as CD69, long lived Trm cells may also be distinguished by their memory phenotype (45). Using CD45RA and CCR7 to distinguish naïve ($CD45RA^+CCR7^+$), effector memory ($CD45RA^-CCR7^-$) central memory ($CD45RA^-CCR7^+$) and TEMRA ($CD45RA^+CCR7^-$), we find *Mtb* infected human lung is highly enriched for effector memory CD4 and CD8 T-cells, compared

to predominantly naïve cells in matched blood (Fig.**3c**). Moreover, effector memory cells were highest in the $CD69^+$ fraction for both CD4 and CD8 T-cells, while naïve and TEMRA were significantly lower (Suppl.Fig.**5e**). The same was true for $CD103^+$ CD8 but not CD4 T-cells. Strikingly, effector memory T-cells were also highly enriched in the $CD69^-$ fraction compared to naïve cells, which may suggest the presence of Trm in lung tissue that lack CD69, as demonstrated in the mouse model (46).

Next, to assess T-cell functionality, lung homogenate and matched blood samples were non-specifically stimulated with mitogen (PMA and ionomycin), and cytokine production measured by intracellular cytokine staining. Consistent with an enrichment of effector memory cells, a greater proportion of CD4 T-cells isolated from lung tissue produced TNF-α, IFN-γ and IL-17 than cells in circulation; whilst lung CD8 T-cells produced more IFN-γ and IL-17 (Fig.**3d**; data presented on a log scale). In both cases, the increased frequency of IL-17 producing T-cells was the most striking (14.6 and 4.7-fold increase for CD4 and CD8 T-cells respectively), in line with described enrichment of Th17 and Tc17 subsets within the lung (47-49). To examine this in more detail, we sought to examine the frequency of cytokine producing cells co-expressing CD69 and CD103. However, the mitogenic stimulation approach used in this study resulted the upregulation of CD69, despite by-passing the TCR (Suppl.Fig.**6a**) (50), making CD69 expression data difficult to interpret on stimulated cells. CD103 expression, in contrast, was not effected by PMA/ionmycin stimulation (Suppl.Fig.**6b**). The CD103 fraction contained the highest frequency of cytokine producing cells, particularly for IFN-γ and IL-17, of which IL-17 is almost exclusively produced by the $CD103^+$ subset (Suppl.Fig.**6c-d**). This trend was reduced in CD8 T-cells, although IL-17 producing CD8 T-cells were also predominantly $CD103^+$. Overall, these data show

that TB diseased human lung tissue contains T-cells that upregulate surface markers of Trms, are highly enriched for memory subsets, and are highly functional and enriched for IL-17 producing subsets.

HIV infection is associated with decreased functionality in tissue-resident T-cells from TB-infected lungs

HIV co-infection rates were high amongst study participants and, although all participants were taking antiretroviral therapy (ART) at the time of surgery, treated HIV remains an important independent risk factor for TB (51). Therefore, the effect of HIV on lung associated T-cells was evaluated using CD4/CD8 ratios (52). In blood from healthy controls, a median CD4/CD8 ratio of 2.04 was observed, within the expected range of 1.5-2.5 for healthy humans (53). However, HIV infected participants displayed a reduced CD4/CD8 ratio in blood (median 0.93, P=0.004 vs healthy controls) (Suppl.Fig **7a**), suggesting persistent immune deficiency despite ART. In the lung, HIV^- participants and cancer controls in our study displayed a median ratio of 1, lower than the expected value of 2 (31), suggesting immune perturbation in these participants. However, HIV co-infection was associated with highly significant further reduction of the lung CD4/CD8 ratio (0.5, P<0.0001 vs HIV^- participants), indicating an additional profound impact of HIV infection on lung T-cells in these diseased participants (Suppl.Fig.**7b**).

Surprisingly, HIV infection was not associated with a significant decrease in the frequency of cytokine producing cells in either bulk lung CD4 T-cells or matched PBMC (Fig.**4a**). However, when we examined cytokine production according to expression of tissue residency markers within the lung, the frequency of $CD103^+CD69^+$ CD4 T-cells

producing TNF-α, IL-2 and IL-17 and $CD103^{-}CD69^{+}$ CD4 T-cells producing IL-2 and IL-17 was significantly lower in from HIV infected individuals compare to HIV uninfected individuals (Fig.**4b**). Similarly, no differences were observed in blood of bulk lung CD8 T-cells, however only the frequency of TNF-α producing CD8 T-cells was significantly reduced in the fraction expressing tissue resident markers (Suppl.Fig.**8a and b**). Overall, these data show that HIV co-infection leads to persistent skewing of CD4:CD8 ratio in the lung and a deficit in lung T-cell functionality, most notably in IL-2 and IL-17 production.

TB-specific T-cells are enriched in the lung and predominantly $CD103^{-}$ tissue-resident effector memory cells

Having determined that T-cells isolated from TB diseased lung overall retain functionality in terms of cytokine production, we next assessed their responsiveness to TB-specific antigens, using MTB300, a peptide pool of 300 *Mtb* epitopes (54). We compared paired blood and lung samples when available (Fig.**5a**), in addition to all lung samples (Fig.**5b**). In the blood, MTB300 specific responses were detected in 16/17 participants, all of which produced TNF-α (median frequency 0.48% of CD4 T-cells), and a proportion of which also had detectable, but less frequent IFN-γ and IL-2 producing cells (median frequency 0.08% in 10/17 participants and 0.05% in 9/17 participants respectively). IL-17 production was only detected in 6/17 participants analysed (Fig.**5b**). Using the same assay, MTB300 specific CD4 T-cells in matched lung samples were significantly higher, with approximately a 5-fold enrichment of TNF-α producing cells relative to blood (2.39% vs 0.48%, P=0.002), and a 10 fold enrichment in IL-2 (0.5 vs 0.05%, P<0.001; Fig.**5a**). Surprisingly, MTB300 specific cells producing IFN-γ cells were not enriched in the lung. However, MTB300 specific

IL-17^{+} cells do appear to be enriched in the lung. This difference becomes significant when all lung samples are taken into consideration (Fig.**5b**, P=0.04). Moreover, a greater proportion of lung samples contained detectable IL-17 responses compared to the blood (15/19 vs 5/16, P=0.007 by Fishers exact test). It is important to note that, as above, the data are presented on a log scale and IL-17 producing T-cells are detected at a lower frequency than those making TNF-α.

As expected, the majority of cytokine-producing *Mtb*-specific T-cells displayed an effector memory phenotype (Suppl.Fig**.9**). However, despite the fact that CD103^{+} T-cells appeared to be most prolific cytokine producers by non-specific stimulation (Suppl.Fig**.6c-d**), MTB300 responsive cells are almost all CD103^{-}, with the most abundant cytokine production observed in the CD103^{-}CD69^{+} and CD103^{-}CD69^{-} fractions (Fig.**5c**). Surprisingly, given our earlier findings, although the frequency of TB-specific CD4 T-cell responses in HIV+ve participants tended to be lower than HIV-ve participants, these differences were not significant (Suppl.Fig**.10**). In addition to memory markers, T-cells were stained for the forkhead box P3 (FoxP3) transcription, a canonical marker of regulatory T-cells (Tregs). Overall, the lung contained fewer FoxP3^{+} cells than circulation (Suppl.Fig.**11a**), and this was not increased in HIV infected participants (Suppl. Fig.**11b**). However, the frequency of TB-specific CD4 T-cells that express FoxP3 was over 6-fold higher in the lung compared to the blood (2.53% vs 0.38%; P<0.0001, Suppl. Fig.**11c**), with the majority of cells producing TNF-α. Again, these cells lacked CD103 expression, and about 50% express CD69 (Suppl. Fig.**11d**). Although FoxP3 is associated with Tregs, it is also transiently upregulated on activated T-cells (55). Therefore, whilst it is tempting to speculate these data

support an expansion of *Mtb*-specific Tregs in the lung, more work is required to confirm this.

TB specific IL17$^+$ cells correlates with reduced systemic inflammation.

As discussed, the TB infected participants analysed in this study were categorized as having active TB based on the assessment of the operating surgeon and had varying degrees of disease severity that, for practical reasons, was not precisely defined. Therefore, in a subset of participants we measured plasma levels of TNF-α, IL-17A and IL-1β, as these pro-inflammatory cytokines have been shown to directly correlate with TB disease severity in the lung and bacterial burden (56, 57). Both the active and previous TB groups analysed contained participants with elevated levels of these cytokines compared to non-TB controls (Suppl.Fig.**12a and c**). However, this was not true of most participants and suggests a range of disease severity. Next, in participants for whom we had both T-cell and cytokine data, we tested whether the frequency of *Mtb*-specific T-cells were associated with plasma cytokine levels, as a potential indicator of lung disease severity. Surprisingly, we found a significant inverse relationship between the frequency of *Mtb*-specific IL-17$^+$ CD4 T-cells and plasma IL-1β concentration (Fig.**6a**; r=-0.7598; p=0.0175). Similar trends were observed between TB-specific IL-17$^+$ T-cell frequency and TNF-α and IL-17A, however the associations were less strong and not significant (data not shown). Notably, plasma IL-1β did not correlate with the frequency of TB-specific T-cell producing IFN-γ, TNF-α or IL-2 (Fig. **6b-d**). Although the numbers of subjects for whom both cytokine and T-cell data were available were small, this data suggests that IL-17 producing T-cell could be more important *in vivo* than the other cytokines measured.

Exogenous IL-17 and IL-2 are protective in a functional 3D granuloma model

Finally, to determine whether the T cell subsets identified in the clinical study may improve control of *Mtb*, we studied these different cytokines in a functional granuloma model (58), with the researcher uninformed of the clinical findings. Primary human immune cells are infected with luminescent Mtb and then encapsulated in collagen/alginate microspheres, within which granuloma-like structures self-aggregate that recapitulate many features of human lung granuloma (58-60). Microspheres were generated using PBMC from 3 healthy donors and incubated with TNF-α, IFN-γ, IL-2 or IL-17. Consistent with other published work using this model (58, 61), IFN-γ and TNF-α promoted *Mtb* growth over the course of 12 days compared to no cytokine controls (Suppl.Fig.**13a**). By contrast, *Mtb* growth was significantly decreased when the microspheres were incubated in media containing either IL-17 or IL-2 (Fig.**7a-b**). For both cytokines, we observed no clear titration effect and there was no clear evidence of synergism when added together (Suppl.Fig.**13b**). Bacterial growth in the model system is measured by luminesce, and we confirmed the suppressive effect of exogenous IL-17 and IL-2 by CFU on day 15 (Suppl.Fig.**12c**). Finally, to investigate potential mechanisms of Mtb growth inhibition in the microsphere system, we determined the effect of exogenous IL-2 and IL-17 on cell survival and production of nitric oxide (NO), an important anti-microbial factor. Exogenous IL-2 but not IL-17 significantly reduced cell death within Mtb-infected microspheres, as measured by lactate dehydrogenase (LDH) levels on culture supernatant on day 7 (Fig.**7c**). Both IL-17 and IL-2 significantly increased NO production at the same timepoint (Fig.**7d**).

DISCUSSION AND CONCLUDING REMARKS

Multiple studies have demonstrated a crucial protective role for Trm in the immune response to pathogens, and there is an increasing interest in exploiting their potential for improved treatment or vaccine strategies, particularly in TB (28-30). While it is clear that Trms are functionally distinct from circulating T-cell populations, to date studies of Trms in TB have been restricted to animal model systems due to the limitations in the availability of fresh human lung tissues. Here, we show that functional cells expressing Trm markers are present in TB diseased human lung tissue and are highly enriched for IL-17 producing subsets and for *Mtb*-reactive T-cells, including *Mtb*-specific IL-17 producing cells. By focusing on Trm-like subsets, we also find that HIV co-infection impairs both IL-17 and IL-2 production from lung resident T-cells. Although we did not find a significant impact of HIV on Mtb-specific T-cell frequency, these data suggest one mechanism through which HIV increases the risk of developing active TB. The importance of IL-17 in particular is also suggested by the inverse correlation between plasma IL-1β and the frequency of TB-specific IL-17$^+$ CD4 T-cells. Finally, using a 3D-model that mimics aspects of human granuloma, we find that addition of exogenous IL-17 and IL-2 both significantly reduced TB growth, whilst it is enhanced by exogenous TNF-α and IFN-γ. Taken together these data suggest that subsets of Mtb specific T-cell are sequestered in the human lung, are functionally different from those detected in circulation and are likely to play an important role in the immune control of Mtb in this tissue.

It is thought that Trms populate specific tissues and become enriched for particular specificities following pathogen exposure. For example, during influenza in mice, Trm are essential for *in situ* immunity after re-exposure (62, 63), and influenza specific Trm

have been identified in human lung parenchyma (64). The potential protection offered by these cells in TB directly was demonstrated by adoptive transfer experiments in mice (14, 65). These studies show that *Mtb* infection leads to the retention of *Mtb*-specific $CD4^+$ T-cells in the lung and these cells provide superior control of *Mtb* infection when adoptively transferred into susceptible T-cell-deficient hosts compared to blood T-cells from the same animal. Although these studies did not examine tissue residency markers, we initially hypothesised that *Mtb* specific Trm would express CD103, partly because epithelial macrophages in TB granuloma upregulate E-cadherin, the ligand for the integrin αEβ7 formed by CD103 and ITGB7 (66). However, our finding that *Mtb* specific T-cells in our TB lung homogenate are almost exclusively CD103-ve is consistent with recent work showing that *Mtb*-antigen specific Trm cells induced by vaccination in the mouse lung expressed low levels of CD103 (67).

The presence of Th17 Trm-like subsets in TB infected human lung is supported by the Cytof analysis. Phenotypically Th17 cells are defined by surface expression CCR6 and CCR4, and *Mtb*-specific T-cells in blood that produce IL-17 express these markers (40). CD161 has also been described as a surface marker that distinguishes Th17 expressing the RoR-γT transcription factor (68), and $CD3^+CD161^+$ IL-17 producing T-cells have been detected in human bronchioalveolar lavage fluid (41). In addition, co-expression of CD39 and CD161 has been associated with driving Th17 polarization in the gut mucosa (69) and CD39 expression by Th17 cells was found to enhance their resistance to inflammation induced cell death through conversion of extracellular ATP (70). Therefore, the distinct $CD69^+$, T-cell subsets in the lung that co-expresses CCR6, CCR4, CD161 and CD39 may represent an important lung Th17 subset. Interestingly, in a mouse model of colitis, this $CD39^+$ Th17 subset plays an important role in resolving

inflammation through production of IL-10. Over-expression of IL-17 is generally seen as detrimental to the *Mtb* immune response (71). However, T-cell production of IL-10, particularly in combination with IL-17, has been associated with sterilizing immunity at granuloma level in NHPs (72). In addition to Th17 cells, Th1* cells can produce IL-17 in response to *Mtb* antigen (73). We did not distinguish IL-17 producing subset in our stimulation experiments and thus either or both Th17 and Th1* cells maybe involved, Moreover, CXCR3 is expressed by some cells within the potential Th17 Trm cluster revealed by Cytof, which is more associated with Th1 rather than Th17 subsets (49). Further work is needed to investigate lung Th17 and Th1* subsets and to explore the potential involvement of additional cytokines including IL10. Although we do not find evidence for a protective role for IFN-γ and TNF-α in this study, a wealth of data indicates that complete loss of the cytokines renders both animals and humans highly susceptible of Mtb (7). Conversely, elegant studies in mice and NHP from Dan Barber's group show that the loss of immune control in the lung associated with interference in the PD-1 immune checkpoint axis is directly related to excessive production of IFN-γ and TNF-α (most recently (74)). Thus, whilst these data and a growing number of studies suggest an important role for IL-17 in the immune response to Mtb, it is highly likely that a balanced immune response is still required (75).

The fact that treated HIV co-infection is associated with reduced IL-17 producing T-cells in the lung is consistent with observations of selective depletion of Th17 from other mucosal compartments, including the gut (76, 77) and female genital tract (78). Failure of ART to restore IL-17 producing T-cells in the female genital tract and the gut mucosa, despite successful reconstitution in the blood, has been linked to reduced CCL20 levels for recruiting Th17 via CCR6 (78, 79). However, it is important to note

that, in one of the above studies, Th17 were found not to be depleted from bronchioalveolar lavage (BAL) fluid of HIV infected participants (77). Likewise, other groups have described reduced TB-specific CD4+ T-cells in BAL cells of HIV coinfected participants compared to non-infected controls (80, 81). In contrast, we did not find a significant reduction in the frequency of TB-specific CD4 lung T-cells in HIV infected participants. More recently, however, the decreased frequency of TB-specific CD4 T-cells in BAL of HIV infected participants was attributed to a large influx of T-cells into the BAL (82). When this was accounted for, HIV infection was actually found to have no impact on the absolute number of TB-specific T-cells in BAL. These finding suggest challenges in comparing the observations from human BAL and tissue and may be consistent with our observed lack of depletion *Mtb* specific CD4 lung T-cells in HIV co-infected participants. The highly skewed CD4:CD8 ratio observed in the lung of HIV infected participants is also consistent with data from humanized mice and NHPs showing profound depletion of parenchymal CD4 T-cells from the lung (44). This was associated with high expression of the HIV co-receptor, CCR5, which our Cytof data shows is highly expressed in lung T-cells.

The observation that lung IL-17 production may play an important role in the immune containment of *Mtb* in the lung is consistent with several recent studies. The IL-17/IL-23 pathway is important for clearance of intracellular bacteria (83, 84) and it appears to be modulated during *Mtb* infection (85, 86). Protection of NHPs by pulmonary BCG vaccination was associated with lung TB-specific Th17 cells, and these were identified as the main correlate of protection (87). Interestingly, protection in this system was also associated with IL-10 production, which the authors speculate may derive from IL-10 producing Th17 cells, although this was not formally measured. In a separate

NHP study, asymptomatic TB infection was associated with *Mtb* specific IL-17 producing T-cells in the BAL that were not detected in the blood (88). Moreover, lung resident Th17 cells were identified as the key mediator of vaccine efficacy in a novel CysVac2/Advax mucosal TB vaccine of mice (67). In humans, high dimensional profiling of blood from a large cohort of TB resistors and progressors in Peru revealed a persistent deficiency in polyfunctional Th17 T-cells in participants who went on to develop active disease (89). Therefore, tissue IL-17 responses are emerging as critical in the host immune response to *Mtb*. To investigate potential mechanisms, we tested whether exogenous IL-17 in the 3D granuloma model system affected cell survival, which may have an indirect effect on Mtb growth, or a more direct effect through the production of NO. IL-2 promoted cell survival in Mtb infected microspheres, which may contribute the protective effect of this cytokine. This was not observed for IL-17, but both cytokines promoted NO production. This is a key molecule in immune defense against Mtb, as shown in animal models using both chemical inhibition and genetic knock out of iNOS, the enzyme that produces NO (90). IL-17 has been shown to induce NO both in vitro and in vivo (91-93), as can IL-2 (94). Interestingly, NO was found to limit Mtb growth in mice be blocking IL-1β ecruitment of granulocytes to the site of disease (95), suggesting a potential mechanistic relationship between IL-17, NO and IL-1β. Whether these in vitro observations are important in vivo is not clear from these data and further work is needed to understand the potential mechanisms.

There are several important caveats to this study that should be considered. All participants underwent surgical lung resection, and therefore should be classified as having failed TB immunity. This is due to the nature of the study cohort and could not be avoided. However, data from NHPs demonstrates that both controlling and non-

controlling granuloma co-exist in the same lung (72). In addition, before antibiotics, ~50% of participants with active TB eventually self-healed through their immune response (96). Therefore, it seems likely that protective immune responses are still present in the lung of participants with progressive TB disease, even though they have failed to protect the whole organism. In this current study, multiple sections from different parts of the same lung were pooled to obtain sufficient cell numbers. In future studies it will be informative to analyse different sections/granuloma from the same lung tissue to formally test if TB adaptive immunity can vary locally. In addition, completely disease free lung samples are simply unavailable and we relied on non-TB infected participants having surgery to remove lung tumours to generate control tissue. Although macroscopically healthy tissue was sampled, T-cell phenotypes may be affected by the adjacent tumour mass. However, our phenotypic observations are in-line with other recent work that studied human lung tissue (24). Finally, the use of plasma cytokines as a proxy marker of disease severity is imprecise and may relate to other sequalae such as bronchiectasis. However, IL-1β was recently identified as the strongest cytokine marker of radiographic extent of TB disease, presence of large cavities and TB smear grade in a clinical trail (57), indicating potential to use as correlate of disease severity. In addition, the fact that these in vivo correlations suggesting an important role for IL-17 is backed up by our *in vitro* model, and by the recent publications highlighted above, strongly suggest that the observations are relevant.

Therefore, in conclusion, despite these limitations, we believe studies such as this, which characterize local tissue-resident immune responses, provide an invaluable resource in terms of understanding the human immune response toward *Mtb*. To the

best of our knowledge, this is the first study in human TB study to provide support for a protective role for lung tissue resident T-cells producing IL-17. This adds strong support to growing evidence from animal models that tissue resident Th17 T-cell responses are likely to be crucial to TB immunity and should be a key target for novel vaccine strategies.

METHODS

Participants

Whole blood was collected in tubes containing EDTA to prevent coagulation. Lung tissue was obtained from the King Dinizulu and Inkosi Albert Luthuli Central Hospitals in Durban, KwaZulu-Natal. Study participants included underwent surgically indicated pulmonary resections due to TB sequalae, which included either bronchiectasis, haemoptysis, recurrent chest infections, drug resistant TB. All subjects undergoing surgery for TB sequalae were classified by the operating surgical team as having either suspected active TB or previous TB infection. This definition was based on clinical history, and a review by the surgical team of pre-operative chest x-ray and CT scans. Of 40 subjects with suspected ATB studied 14 had matched histological information, of which 11 had indicative fibrocaseous or necrotising granuloma and 2 had detectable acid-fast bacilli. With the exception of emergency surgeries, all individuals undergoing lung surgery are placed on a minimum of 2 weeks of anti-TB drug therapy (usually Rifafour) to minimize risk to the operating surgeons, and this Mtb culture on tissue sample was not attempted. Control samples were obtained from macroscopically normal lung tissue from participants who underwent pulmonary resection for lung cancer. All participants provided informed consent and the study was approved by the Biomedical Research Ethics Committee.

Sample preparation

Peripheral blood mononuclear cells (PBMCs) were isolated from whole blood using the Ficoll-Histopaque (Sigma) density gradient centrifugation and used fresh in assays or frozen in liquid nitrogen in freezing media (90% FBS containing 10% DMSO). Where frozen PBMCs were used, samples were thawed in DNase (Roche) -containing (25 units/ml) R10 which had been pre-heated to 37°C. Cells were rinsed and rested at 37°C overnight before assay set up.

Resected tissues were dissected and washed several times with cold HBSS (Lonza) before being re-suspended in 8mls of pre-warmed digestion media R10 (RPMI supplemented with 10% FCS, 2 mM L-glutamate, 100 U/ml Penstrep), containing 0.5 mg/ml collagenase D (Roche) and 40 U/ml DNaseI (Roche), and transferred to GentleMACS C-tubes (Miltenyi) for mechanical digestion per manufacturer's instructions. The resultant suspension was incubated for 30 minutes at 37° C, subjected to an additional mechanical digestion step followed by another 30-minute incubation step at 37°C. The final suspension was strained through a 70 µm cell strainer, and washed twice in HBSS. Following this step cells were rested at 37°C overnight and lysed before counting in TC20™Automated Cell Counter (Bio-Rad) and assay set up.

Mass cytometry staining and data analysis

Lung cells were counted and stained in 100µl containing APC-CD45 (1:20) and incubated on ice for 20 mins. Cells were washed then resuspended in 100µl cold cyFACS buffer. PBMCs were counted in 1ml of cold cyFACS buffer and a maximum

of $3x10^6$ live cells resuspended in 100µl of cold cyFACS buffer. Both lung cells and PBMC were kept on ice throughout the staining process. For participants with matched tissue and blood, 100µl APC-CD45 positive lung cells was mixed with 100µl of matched PBMC. The total number of cells stained varied between 3 – $5x10^6$. The samples were washed once then resuspended in 100µl of freshly diluted cisplatin (200 µM), for discrimination of live and dead cells, and incubated on ice for 5 minutes. Cells were washed and resuspended in 50µl of cyFACS buffer containing surface primary antibody cocktail and incubated at 37^{o}C for 15 minutes. After washing, cells were then incubated with a secondary antibody cocktail (including the metal labelled anti-fluorochrome antibody for the detection of live cell barcoded tissue samples) for 30 min on ice followed by fixing the cells in 2% paraformaldehyde in PBS overnight at 4^{o}C. The next day the cells were washed, resuspended in freezing medium (90%FBS, 10% DMSO) and frozen later for CyTOF acquisition. After thawing, cells were further stained for panel specific intracellular markers and DNA and each sample was barcoded with a unique combination of two distinct cellular barcodes (97). Cells were washed and adjusted to 0.5 million cells per ml H_2O together with 1% equilibration beads (EQ Four element calibration beads, Fluidigm) for acquisition on a CyTOF® Helios system.

Signals for each parameter were normalized based on EQ beads added to each sample. Any zero values were randomized using a custom R-script that uniformly distributes values between minus-one and zero. Each sample was manually de-barcoded followed by gating on DNA+ cells. Immune cells were identified by gating on live (cisplatin-) CD45+ cells and tissue and PBMCs from the same donor were further identified according to the tissue-specific live cell barcode tag (APC-CD45). Subset

identification followed a gating cascade according to the lineage markers using FlowJo (Tree Star Inc) software. High dimensional data analysis was performed using immunoSCAPE's cloud-based analytical pipeline tool Cytographer®. For the visualization of high dimensionality data, Uniform Manifold Approximation and Projection (UMAP) as dimensionality reduction technique (98) was used. Phenotypic dissection was performed using the PhenoGraph clustering algorithm (99). Marker expression intensities were represented as heatmaps and expression plots. Dot plots and UMAP plots were displayed using Flowjo.

Intracellular cytokine transcription factor staining

Lung cells and PMBCs were plated in each well of a round bottom 96-well plate and incubated in the presence of MTB300 peptide (2ug/ml; La Jolla Institute of Immunology). Incubation in the presence of mixture of PMA (0.5uL/200uL) and Ionomycin (0.3uL/200uL) or in the absence of stimuli were used as positive and negative controls, respectively. Cells were incubated for 1 h at 37° C, at which point Golgi Stop solution and Golgi Plug (BD Biosciences) was added to each well for the remaining 4 h.

Flow Cytometry

For all experiments, identification of immune cells was done by surface staining with a near-infrared live/dead cell viability cell staining kit (Invitrogen) and a combination of the following fluorochrome conjugated antibodies: αCD45-V500 Horizon clone HI30 (BD Biosciences), αCD3 Brilliant Violet 785 clone OKT3 (Biolegend), αCD4 Brilliant Ultra Violet 496 clone SK3 (BD Bioscience), αCD8 Brilliant Violet 605 clone RPA-T8 (Biolegend), αCD19-FITC clone HIB19 (BD Bioscience), αCD62L-PE-Cy5 clone

DREG-56 (BD Biosciences), αCD103-APC clone Ber-ACT8 (BD Biosciences), αCD45RA Brilliant Violet 650 clone HI100 (BD Biosciences), αCCR7 – PerCP-Cy5.5 clone G043H7 (Biolegend), αCD25 Brilliant Violet 711clone BC96 (Biolegend), αCD56 Brilliant Violet 711 clone HCD56(BioLegend), αCD16 Brilliant Violet 650 clone 3G8 (BioLegend), αCD69 Brilliant Ultra Violet 395 clone FN50 (Brilliant Horizon), αPD-1 Brilliant Violet 421 clone EH12.1 (BD Biosciences), αCTLA-4 PE L3D10 (Biolegend), αTIM-3 Alexa 700 clone 344823 (R&D Systems). Cells were surface stained with 25uL of antibody cocktail in the dark for 20 minutes at room temperature followed by washing with PBS. Where intracellular staining was not performed, cells were immediately fixed with 2% paraformaldehyde then acquired on FACSARIA Fusion (BD).

For intracellular cytokine staining, surface stain was washed off and cells were permeabilized using Fix/Perm kit (BD Biosciences) for 20 minutes at 4^{o}C washed and 20% goat serum added for 20 minutes at room temperature in the dark to block non-specific antibody binding. Following a washing step, 25uL of the following cytokine cocktail was added: αTNFα Alexa700 clone Mab11 (BD Biosciences), αIL-2 PE-CF594 clone 5344.111 (BD Biosciennces), αIFN-γ PE-Cy7 clone 4S.B3 BD Biosciences or Brilliant Violet 421 clone 4S.B3 (Biolegend), αIL-17 PE clone BL168 (Biolegend).

For measurement of transcription factor FoxP3, the eBioscience Fixation/Permeabilization kit (eBioscience) was used for intracellular staining the blocked blocked with 20% goat serum for 20 mins prior to antibody staining with αFoxP3 eFlour 450 clone PCH101(eBioscience). Data acquisition was performed

using Aria Fusion or Aria III cytometers (BD) and analyzed using FlowJo Software v.9.9 (Treestar Inc, Ashland, OR).

Plasma Cytokine Analysis

Plasma samples were collected from whole blood and frozen at –80^{o}C until when needed. TNF-α, IL-17A, IL1- β levels were quantified using a multi-plex high-sensitivity Milliplex Map Kits (Millipore) on a Bio-Plex 200 system (Bio-Rad) using manufacturer's instructions.

Cell encapsulation to form 3-D culture microspheres

Microspheres were generated as previously described (58, 60). Peripheral blood mononuclear cells (PBMCs) were isolated using density gradient centrifugation over Ficoll-Paque (GE Healthcare Life Sciences, UK) from apparently healthy blood donors (Ethical approval ref. 13/SC/0043). Bioluminescent *Mycobacterium tuberculosis* H37Rv were routinely cultured in Middlebrook 7H9 medium (BD Biosciences, Oxford) supplemented with 10% ADC enrichment (SLS), 0.2% glycerol and 0.02% Tween 80 with kanamycin (25µg/ml). For all experiments, bacterial cultures were grown to optical density of 0.6 (approx. 1x 10^8 CFU/ml). Host cells were then infected with luminescent mycobacteria at a multiplicity of infection (MOI) of 0.1. After overnight incubation at 37°C in 5% CO_2, the infected PBMCs were treated with Versene solution for 10 min and neutralised by HBSS without Ca/Mg (Gibco). The cells were detached by scraping, placed in 50ml falcon tubes, topped up with HBSS and spun at 320 x g for 8 min at 4°C. To obtain a 3-D culture, we re-suspended *Mtb*-infected host cells in sterile alginate-collagen matrix at 5 x 10^6 cells per ml. The mix was injected into the Electrostatic Bead Generator (Nisco, Zurich, Switzerland) to form microspheres via a

Harvard syringe driver as described previously (100). After washing two times in HBSS without Ca/Mg (Gibco) they were equally distributed into 2ml Eppendorfs and immersed in 1ml RPMI medium (consisting of RPMI 1640 medium supplemented with 10µg/ml of ampicillin, 2mM of glutamine, 25µg/ml of kanamycin and 10% of human AB serum) with or without cytokines and incubated at 37°C and 5% CO_2. We monitored bacterial bioluminescence using a GloMax® 20/20 Luminometer. All the cytokines are purchased from ImmunoTools (Germany), suspended in RPMI with 0.1% human serum and kept at -80^{O}C until use. The cytokines include IL-2, IL-17A, TNF-α and IFN-γ. A 250ul of media were taken and replaced with equal amount of the media with or without four times of the cytokine concentration. Bacterial growth was monitored with luminescence using GloMax® Discover microplate reader (Promega,UK). Cell viability in microspheres was determined by Lactate Dehydrogenase (LDH) release in the supernatants collected at day seven. This was analysed by a colorimetric activity assay as per manufacturer's instructions (Roche, Burgess Hill, United Kingdom). LDH was quantified using LDH standards provided and results were normalized using levels in from microspheres with no cytokine in each experiment. NO production in microspheres was determined by detection of accumulated nitrites (NO2 −) in the cell supernatants using the Griess reagent system (Promega) according to the manufacturer's instructions. Briefly, 100 µl of the cell supernatant was incubated with 100 µl Griess reagent (Promega) for 15 min in a dark at room temperature and the absorbance was measured at 546 nm on a GloMax Discover UV/Vis microplate reader (Promega). The concentrations of nitrites were derived by regression analysis using serial dilutions of sodium nitrite as a standard and normalized with the amount from microspheres with no cytokine for each experiment.

Statistical Analysis

All statistical analyses were performed using GraphPad Prism version 6.0d (GraphPad Software, Inc.) Comparisons of two groups were done by a paired or unpaired student's t-test (Wilcoxon test or Mann-Whitney test respectively) where a P-value of 0.05 and below was statistically significant. Significance of more than two groups was determined using a Kruskal-Wallis test or where specific comparisons between two or more groups were relevant, a Mann-Whitney test with Bonferroni correction for multiple comparison was done. P-values of $p<0.05$ are shown, with values that passed correction for multiple comparisons highlighted with *.

Study approval

All participants provided informed consent, and the study was approved by the Biomedical Research Ethics Committee (BREC) of the University of KwaZulu-Natal (BE019/13).

Author Contributions

PO conducted all flow experiments and assisted with data analysis and writing of the manuscript; LBK carried out all 3D model experiments; AA, SN, ANgO conducted CyTOF studies, assisted sample preparation; MF, BL, AN FK, KK, KJD, IA, and RM obtained samples and analyzed clinical information; CSLA, AS provided MTB300, AJCS established the lung cohort; HK and PE helped with data interpretation, study design and manuscript preparation; AL is the senior author who designed and implemented this study, analyzed the data, and co-wrote the manuscript with PO.

References

1. Harding, E. News WHO global progress report on tuberculosis elimination. *The Lancet Respiratory medicine* 1–1 2019. doi:10.1016/S2213-2600(19)30418-7.

2. Young D, Dye C. The development and impact of tuberculosis vaccines. *Cell* 2006;124(4):683–687.

3. Cohen A, Mathiasen VD, Schön T, Wejse C. The global prevalence of latent tuberculosis: a systematic review and meta-analysis. *Eur Respir J* 2019;54(3). doi:10.1183/13993003.00655-2019

4. Jeyanathan M, Yao Y, Afkhami S, Smaill F, Xing Z. New Tuberculosis Vaccine Strategies: Taking Aim at Un-Natural Immunity. *Trends Immunol.* 2018;39(5):419–433.

5. Orme IM. A new unifying theory of the pathogenesis of tuberculosis. *Tuberculosis (Edinb)* 2014;94(1):8–14.

6. Flynn JL. Immunology of tuberculosis and implications in vaccine development. *Tuberculosis* 2004;84(1-2):93–101.

7. O'Garra A et al. The Immune Response in Tuberculosis. *Annu. Rev. Immunol.* 2013;31(1):475–527.

8. Jasenosky LD, Scriba TJ, Hanekom WA, Goldfeld AE. T cells and adaptive immunity to Mycobacterium tuberculosis in humans. *Immunol. Rev.* 2015;264(1):74–87.

9. Torrado E, Cooper AM. IL-17 and Th17 cells in tuberculosis. *Cytokine & Growth Factor Reviews* 2010;21(6):455–462.

10. Cooper AM, Flynn JL. The protective immune response to Mycobacterium tuberculosis. *Curr. Opin. Immunol.* 1995;7(4):512–516.

11. Flynn JL, Chan J. Immunology of tuberculosis. *Annu. Rev. Immunol.* 2001;19:93–129.

12. Takamura S et al. Specific niches for lung-resident memory CD8 +T cells at the site of tissue regeneration enable CD69-independent maintenance. *Journal of Experimental Medicine* 2016;213(13):3057–3073.

13. Steinert EM et al. Quantifying Memory CD8 T Cells Reveals Regionalization of Immunosurveillance. *Cell* 2015;161(4):737–749.

14. Sakai S et al. Cutting Edge: Control of Mycobacterium tuberculosis Infection by a Subset of Lung Parenchyma-Homing CD4 T Cells. *The Journal of Immunology* 2014;192(7):2965–2969.

15. Beura LK et al. Lymphocytic choriomeningitis virus persistence promotes effector-like memory differentiation and enhances mucosal T cell distribution. *J. Leukoc. Biol.* 2015;97(2):217–225.

16. Cauley LS, Lefrançois L. Guarding the perimeter: protection of the mucosa by tissue-resident memory T cells. *Mucosal Immunol* 2013;6(1):14–23.

17. Mueller SN, Gebhardt T, Carbone FR, Heath WR. Memory T cell subsets, migration patterns, and tissue residence. *Annu. Rev. Immunol.* 2013;31:137–161.

18. Ariotti S, Haanen JB, Schumacher TN. Behavior and function of tissue-resident memory T cells. *Adv Immunol* 2012;114:203–216.

19. Mueller SN, Mackay LK. Tissue-resident memory T cells: local specialists in immune defence. *Nat. Rev. Immunol.* 2015;16(2):79–89.

20. Masopust D, Vezys V, Marzo AL, Lefrançois L. *Pillars article: preferential localization of effector memory cells in nonlymphoid tissue. Science. 2001. 291: 2413-2417.* J Immunol; 2014:

21. Schenkel JM, Masopust D. Tissue-Resident Memory T Cells. *IMMUNI* 2014;41(6):886–897.

22. Gebhardt T, Mackay LK. Local immunity by tissue-resident CD8(+) memory T cells. *Front. Immunol.* 2012;3:340.

23. Park CO, Kupper TS. The emerging role of resident memory T cells in protective immunity and inflammatory disease. *Nat Med* 2015;21(7):688–697.

24. Kumar BV et al. Human Tissue-Resident Memory T Cells Are Defined by Core Transcriptional and Functional Signatures in Lymphoid and Mucosal Sites. *CellReports* 2017;20(12):2921–2934.

25. Ogongo P, Porterfield JZ, Leslie A. Lung Tissue Resident Memory T-Cells in the Immune Response to Mycobacterium tuberculosis. *Front. Immunol.* 2019;10:419–11.

26. Perdomo C et al. Mucosal BCG Vaccination Induces Protective Lung-Resident Memory T Cell Populations against Tuberculosis. *MBio* 2016;7(6). doi:10.1128/mBio.01686-16

27. Bull NC et al. Enhanced protection conferred by mucosal BCG vaccination associates with presence of antigen-specific lung tissue-resident PD-1+ KLRG1- CD4+ T cells. *Mucosal Immunol* 2019;12(2):555–564.

28. Kaushal D et al. Mucosal vaccination with attenuated Mycobacterium tuberculosis induces strong central memory responses and protects against tuberculosis. *Nat Commun* 2015;6(1):8533–14.

29. Aguilo N et al. Pulmonary Mycobacterium bovis BCG vaccination confers dose-dependent superior protection compared to that of subcutaneous vaccination. *Clin Vaccine Immunol* 2014;21(4):594–597.

30. Flórido M et al. Pulmonary immunization with a recombinant influenza A virus vaccine induces lung-resident CD4+ memory T cells that are associated with protection against tuberculosis. *Mucosal Immunol* 2018;11(6):1743–1752.

31. Sathaliyawala T et al. Distribution and Compartmentalization of Human Circulating and Tissue-Resident Memory T Cell Subsets. *IMMUNI* 2013;38(1):187–197.

32. Schenkel JM, Fraser KA, Masopust D. Cutting edge: resident memory CD8 T cells occupy frontline niches in secondary lymphoid organs. *The Journal of Immunology* 2014;192(7):2961–2964.

33. Hombrink P et al. Programs for the persistence, vigilance and control of human CD8+ lung-resident memory T cells. *Nat. Immunol.* 2016;17(12):1467–1478.

34. Kloverpris HN et al. Innate Lymphoid Cells Are Depleted Irreversibly during Acute HIV-1 Infection in the Absence of Viral Suppression. *Immunity* 2016;44(2):391–405.

35. Beura LK et al. Intravital mucosal imaging of CD8+ resident memory T cells shows tissue-autonomous recall responses that amplify secondary memory. *Nat. Immunol.* 2018;19(2):173–182.

36. Gordon CL et al. Tissue reservoirs of antiviral T cell immunity in persistent human CMV infection. *Journal of Experimental Medicine* 2017;214(3):651–667.

37. Oja AE et al. Trigger-happy resident memory CD4+ T cells inhabit the human lungs. *Mucosal Immunol* 2018;11(3):654–667.

38. Godefroy E, Zhong H, Pham P, Friedman D, Yazdanbakhsh K. TIGIT-positive circulating follicular helper T cells display robust B-cell help functions: potential role in sickle cell alloimmunization. *Haematologica* 2015;100(11):1415–1425.

39. Slight SR et al. CXCR5+ T helper cells mediate protective immunity against tuberculosis. *J. Clin. Invest.* 2013;179:5099–15.

40. Acosta-Rodriguez EV et al. Surface phenotype and antigenic specificity of human interleukin 17–producing T helper memory cells. *Nat. Immunol.* 2007;8(6):639–646.

41. Gonzalez Y et al. CD161 Expression Defines a Th1/Th17 Polyfunctional Subset of Resident Memory T Lymphocytes in Bronchoalveolar Cells. *PLoS ONE* 2015;10(4):e0123591–13.

42. Zhao H, Bo C, Kang Y, Li H. What Else Can CD39 Tell Us? *Front. Immunol.* 2017;8:727.

43. Woodward Davis AS et al. The human tissue-resident CCR5+ T cell compartment maintains protective and functional properties during inflammation. *Science Translational Medicine* 2019;11(521). doi:10.1126/scitranslmed.aaw8718

44. Corleis B et al. HIV-1 and SIV Infection Are Associated with Early Loss of Lung Interstitial CD4+ T Cells and Dissemination of Pulmonary Tuberculosis. *Cell Reports* 2019;26(6):1409–1418.e5.

45. Sallusto F, Lenig D, Förster R, Lipp M, Lanzavecchia A. Two subsets of memory T lymphocytes with distinct homing potentials and effector functions. *Nature* 1999;401(6754):708–712.

46. Topham DJ, Reilly EC. Tissue-Resident Memory CD8+ T Cells: From Phenotype to Function. *Front Immunol* 2018 Mar 26;9:515. doi: 10.3389/fimmu.2018.00515.

47. Hamada H et al. Tc17, a unique subset of CD8 T cells that can protect against lethal influenza challenge. *The Journal of Immunology* 2009;182(6):3469–3481.

48. Chang SH et al. T helper 17 cells play a critical pathogenic role in lung cancer. *Proceedings of the National Academy of Sciences* 2014;111(15):5664–5669.

49. Nikitina IY et al. Th1, Th17, and Th1Th17 Lymphocytes during Tuberculosis: Th1 Lymphocytes Predominate and Appear as Low-Differentiated CXCR3+CCR6+ Cells in the Blood and Highly Differentiated CXCR3+/-CCR6- Cells in the Lungs. *The Journal of Immunology* 2018;200(6):2090–2103.

50. Cibrián D, Sánchez-Madrid F. CD69: from activation marker to metabolic gatekeeper. *Eur. J. Immunol.* 2017;47(6):946–953.

51. Fenner L et al. HIV viral load as an independent risk factor for tuberculosis in South Africa: collaborative analysis of cohort studies. *J Int AIDS Soc* 2017;20(1):21327.

52. Trickey A et al. CD4:CD8 Ratio and CD8 Count as Prognostic Markers for Mortality in Human Immunodeficiency Virus-Infected Patients on Antiretroviral Therapy: The Antiretroviral Therapy Cohort Collaboration (ART-CC). *Clin. Infect. Dis.* 2017;65(6):959–966.

53. McBride JA, Striker R. Imbalance in the game of T cells: What can the CD4/CD8 T-cell ratio tell us about HIV and health? *PLoS Pathog.* 2017;13(11):e1006624.

54. Lindestam Arlehamn CS et al. A Quantitative Analysis of Complexity of Human Pathogen-Specific CD4 T Cell Responses in Healthy M. tuberculosis Infected South Africans. *PLoS Pathog.* 2016;12(7):e1005760–27.

55. Wang J, Ioan-Facsinay A, van der Voort EIH, Huizinga TWJ, Toes REM. Transient expression of FOXP3 in human activated nonregulatory CD4+ T cells. *Eur. J. Immunol.* 2007;37(1):129–138.

56. Kumar NP, Moideen K, Banurekha VV, Nair D, Babu S. Plasma Proinflammatory Cytokines Are Markers of Disease Severity and Bacterial Burden in Pulmonary Tuberculosis. *Open Forum Infect Dis* 2019;6(7):ofz257.

57. Sigal GB et al. Biomarkers of Tuberculosis Severity and Treatment Effect: A Directed Screen of 70 Host Markers in a Randomized Clinical Trial. *EBioMedicine* 2017;25(C):112–121.

58. Tezera LB et al. Dissection of the host-pathogen interaction in human tuberculosis using a bioengineered 3-dimensional model. *eLife* 2017;6. doi:10.7554/eLife.21283

59. Shammari Al B et al. The Extracellular Matrix Regulates Granuloma Necrosis in Tuberculosis. *Journal of Infectious Diseases* 2015;212(3):463–473.

60. Bielecka MK et al. A Bioengineered Three-Dimensional Cell Culture Platform Integrated with Microfluidics To Address Antimicrobial Resistance in Tuberculosis. *MBio* 2017;8(1). doi:10.1128/mBio.02073-16

61. Tezera LB et al. Anti-PD-1 immunotherapy leads to tuberculosis reactivation via dysregulation of TNF-α. *eLife* 2020;9:463.

62. Teijaro JR et al. Cutting edge: Tissue-retentive lung memory CD4 T cells mediate optimal protection to respiratory virus infection. *The Journal of Immunology* 2011;187(11):5510–5514.

63. Teijaro JR, Verhoeven D, Page CA, Turner D, Farber DL. Memory CD4 T cells direct protective responses to influenza virus in the lungs through helper-independent mechanisms. *J. Virol.* 2010;84(18):9217–9226.

64. Pizzolla A et al. Influenza-specific lung-resident memory T cells are proliferative and polyfunctional and maintain diverse TCR profiles. *Journal of Clinical Investigation* 2018;128(2):721–733.

65. Sakai S et al. CD4 T Cell-Derived IFN-γ Plays a Minimal Role in Control of Pulmonary Mycobacterium tuberculosis Infection and Must Be Actively Repressed by PD-1 to Prevent Lethal Disease. *PLoS Pathog.* 2016;12(5):e1005667–22.

66. Cronan MR et al. Macrophage Epithelial Reprogramming Underlies Mycobacterial Granuloma Formation and Promotes Infection. *Immunity* 2016;45(4):861–876.

67. Counoupas C et al. Mucosal delivery of a multistage subunit vaccine promotes development of lung-resident memory T cells and affords interleukin-17-dependent protection against pulmonary tuberculosis. *npj Vaccines* 2020;5(1):105–12.

68. Maggi L et al. CD161 is a marker of all human IL-17-producing T-cell subsets and is induced by RORC. *Eur. J. Immunol.* 2010;40(8):2174–2181.

69. Bai A et al. CD39 and CD161 Modulate Th17 Responses in Crohn's Disease. *J. Immunol.* 2014;193(7):3366–3377.

70. Fernández D et al. Purinergic Signaling as a Regulator of Th17 Cell Plasticity. *PLoS ONE* 2016;11(6):e0157889–16.

71. Ring S et al. Blocking IL-10 receptor signaling ameliorates Mycobacterium tuberculosis infection during influenza-induced exacerbation. *JCI Insight* 2019;4(10):B38–18.

72. Gideon HP et al. Variability in Tuberculosis Granuloma T Cell Responses Exists, but a Balance of Pro- and Anti-inflammatory Cytokines Is Associated with Sterilization. *PLoS Pathog.* 2015;11(1):e1004603–28.

73. Arlehamn CL et al. Transcriptional Profile of Tuberculosis Antigen–Specific T Cells Reveals Novel Multifunctional Features. *J. Immunol.* 2014;193(6):2931–2940.

74. Kauffman KD et al. PD-1 blockade exacerbates Mycobacterium tuberculosis infection in rhesus macaques. *Sci. Immunol.* 2021;6(55). doi:10.1126/sciimmunol.abf3861

75. Tezera LB, Mansour S, respiratory PEAJO, 2020. Reconsidering the Optimal Immune Response to Mycobacterium tuberculosis. *atsjournals.org* doi:10.1164/rccm.201908-1506PP

76. Pandiyan P et al. Mucosal Regulatory T Cells and T Helper 17 Cells in HIV-Associated Immune Activation. *Front. Immunol.* 2016;7(Suppl 1):787–13.

77. Brenchley JM et al. Differential Th17 CD4 T-cell depletion in pathogenic and nonpathogenic lentiviral infections. *Blood* 2008;112(7):2826–2835.

78. Caruso MP et al. Impact of HIV-ART on the restoration of Th17 and Treg cells in blood and female genital mucosa. *Sci. Rep.* 2019;9(1):1–16.

79. Loiseau C et al. CCR6- regulatory T cells blunt the restoration of gut Th17 cells along the CCR6–CCL20 axis in treated HIV-1-infected individuals. *Mucosal Immunol* 2016;:1–14.

80. Kalsdorf B et al. HIV-1 Infection Impairs the Bronchoalveolar T-Cell Response to Mycobacteria. *Am. J. Respir. Crit. Care Med.* 2009;180(12):1262–1270.

81. Jambo KC et al. Bronchoalveolar CD4+ T cell responses to respiratory antigens are impaired in HIV-infected adults. *Thorax* 2011;66(5):375–382.

82. Bunjun R et al. Effect of HIV on the Frequency and Number of Mycobacterium tuberculosis–Specific CD4+ T Cells in Blood and Airways During Latent M. tuberculosis Infection. *J. Infect. Dis.* 2017;216(12):1550–1560.

83. Gopal R et al. Unexpected Role for IL-17 in Protective Immunity against Hypervirulent Mycobacterium tuberculosis HN878 Infection. *PLoS Pathog.* 2014;10(5):e1004099–14.

84. Khader SA, Gopal R. IL-17 in protective immunity to intracellular pathogens. *Virulence* 2010;1(5):423–427.

85. Shen H, Chen ZW. The crucial roles of Th17-related cytokines/signal pathways in M. tuberculosis infection. *Cell Mol Immunol* 2018;15(3):216–225.

86. Iwanaga N, Kolls JK. Updates on T helper type 17 immunity in respiratory disease. *Immunology* 2019;156(1):3–8.

87. Dijkman K et al. Prevention of tuberculosis infection and disease by local BCG in repeatedly exposed rhesus macaques2019;:1–20.

88. Shanmugasundaram U et al. Pulmonary Mycobacterium tuberculosis control associates with CXCR3- and CCR6-expressing antigen-specific Th1 and Th17 cell recruitment. *JCI Insight* 2020;5(14). doi:10.1172/jci.insight.137858

89. Nathan A et al. Multimodal memory T cell profiling identifies a reduction in a polyfunctional Th17 state associated with tuberculosis progression. *bioRxiv* 2020;:1–46.

90. Jamaati H et al. Nitric Oxide in the Pathogenesis and Treatment of Tuberculosis. *Front Microbiol* 2017;8:436–11.

91. Rafa H et al. IL-23/IL-17A Axis Correlates with the Nitric Oxide Pathway in Inflammatory Bowel Disease: Immunomodulatory Effect of Retinoic Acid. *Journal of Interferon & Cytokine Research* 2013;33(7):355–368.

92. Wang S et al. Interleukin-17 promotes nitric oxide-dependent expression of PD-L1 in mesenchymal stem cells. *Cell & Bioscience* 2020;:1–11.

93. Liu AC, Lee M, McManus BM, Choy JC. Induction of endothelial nitric oxide synthase expression by IL-17 in human vascular endothelial cells: implications for vascular remodeling in transplant vasculopathy. *The Journal of Immunology* 2012;188(3):1544–1550.

94. Wink DA et al. Nitric oxide and redox mechanisms in the immune response. *J. Leukoc. Biol.* 2011;89(6):873–891.

95. Mishra BB et al. Nitric oxide prevents a pathogen-permissive granulocytic inflammation during tuberculosis. *Nature Microbiology* 2017;:1–11.

96. Millington KA, Gooding S, Hinks TSC, Reynolds DJM, Lalvani A. Mycobacterium tuberculosis–Specific Cellular Immune Profiles Suggest Bacillary Persistence Decades after Spontaneous Cure in Untreated Tuberculosis. *J. Infect. Dis.* 2010;202(11):1685–1689.

97. Bodenmiller B et al. Multiplexed mass cytometry profiling of cellular states perturbed by small-molecule regulators. *Nat Biotechnol* 2012;30(9):858–867.

98. Becht E et al. Dimensionality reduction for visualizing single-cell data using UMAP. *Nat Biotechnol* 2018;37(1):38–44.

99. Levine JH et al. Data-Driven Phenotypic Dissection of AML Reveals Progenitor-like Cells that Correlate with Prognosis. *Cell* 2015;162(1):184–197.

100. Tezera LB, Bielecka MK, Elkington PT. Bioelectrospray Methodology for Dissection of the Host-pathogen Interaction in Human Tuberculosis. *Bio Protoc* 2017;7(14):e2418–e2418.

Figures

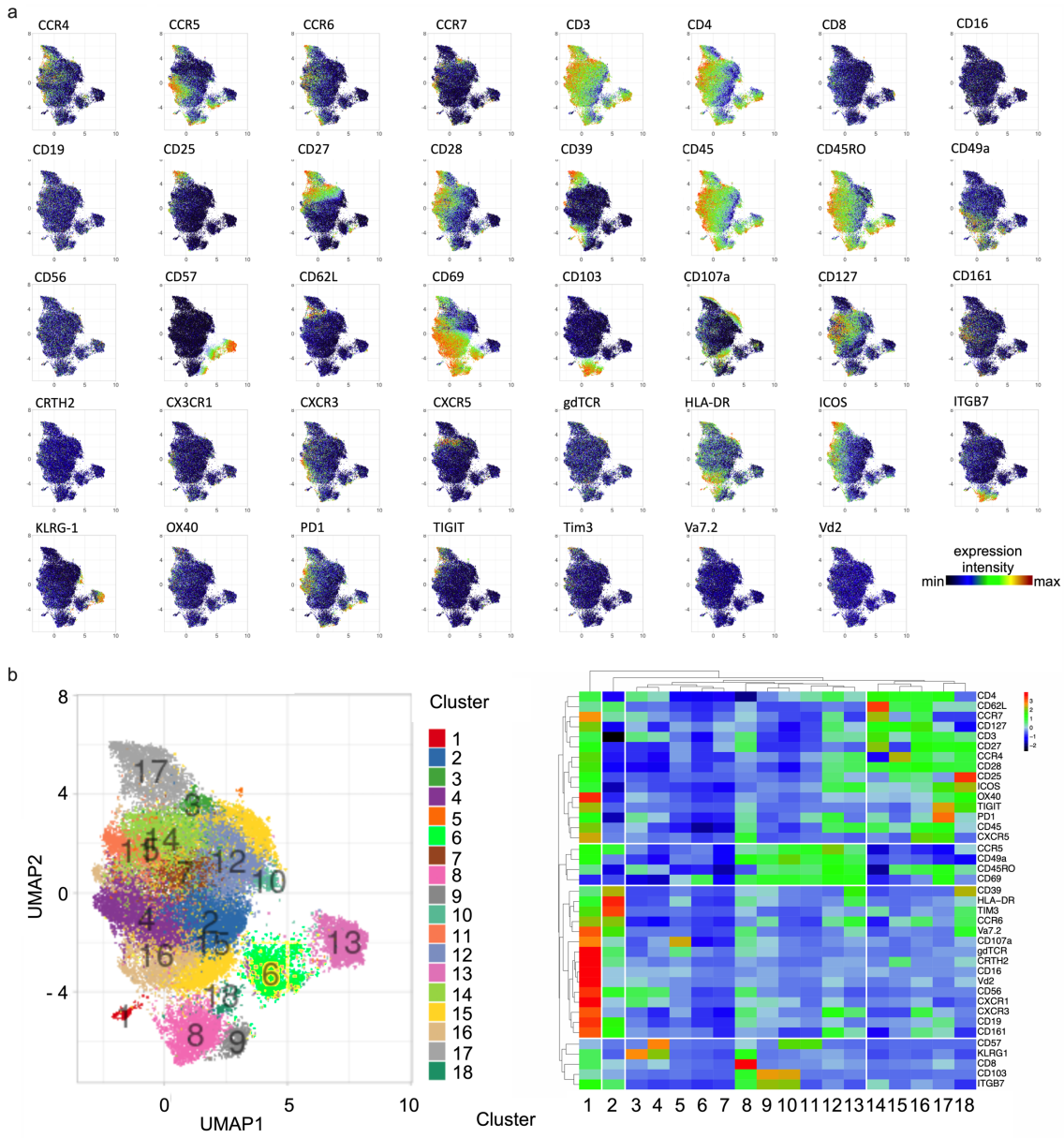

Figure 1. Human lung tissue contains populations of Trm-like T-cells. (a) Cumulative staining of lung CD4 T-cells from 12 biological replicates, defined as having either active TB or previous TB, by CyTOF high dimensional phenotyping based on UMAP plotted as UMAP1 (x-axis) vs UMAP2 (yaxis) for each cell type. (**b**) Phenograph clustering (left) identified 18 clusters (cluster 1-18) depicted on the heatmap of staining intensity of T-cell markers (right).

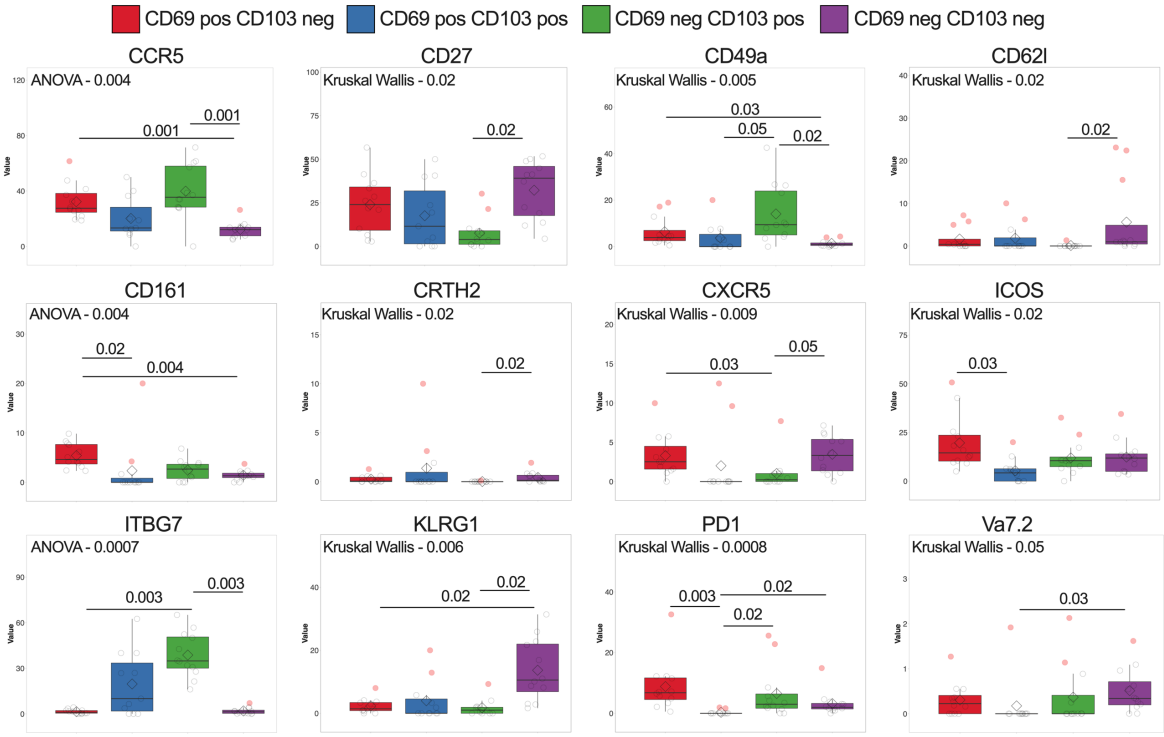

Figure 2. Expression pattern of surface markers in Cytof panel significantly differentially expressed on CD4 T-cells in lung homogenate according to co-expression of CD69 and CD103. Markers not significantly expressed presented in Suppl. Fig. 1.a, significance test applied stated within each individual plot.

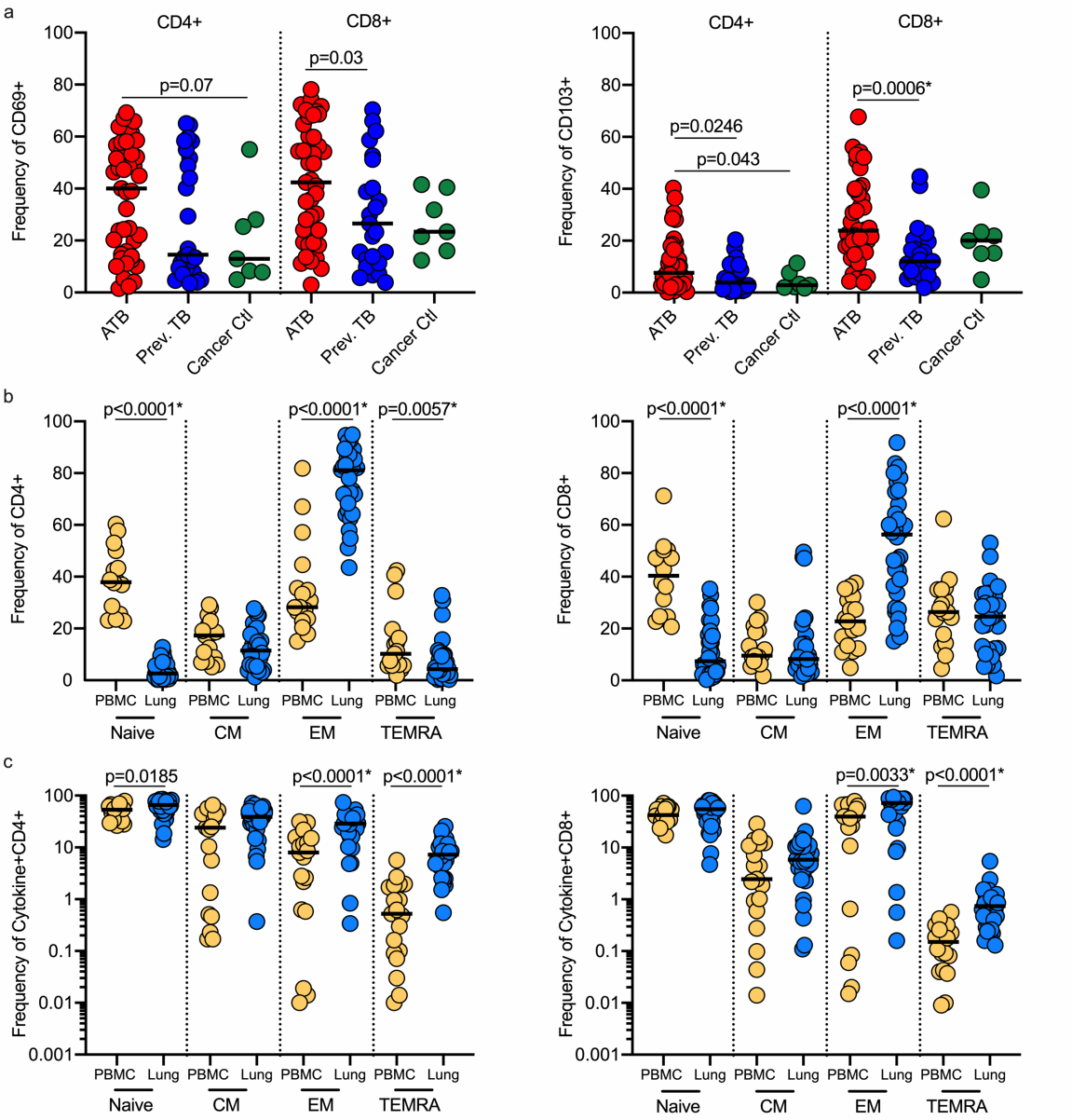

Figure 3. Lung Trm-like T-cells are functional and predominantly effector memory. (a) Frequencies of CD69^{+} CD4 and CD8 T cells isolated from lung tissues from participants with active TB (red), previous TB (dark blue) or cancer controls (dark green). (**b**) Frequencies of CD103^{+} CD4 and CD8 T cells isolated from lung tissues from participants with active TB (red), previous TB (dark blue) or cancer controls (dark green). (**c**) Frequencies of CD4^{+} (left) and CD8^{+}T-cells (right) expressing naïve, central memory (CM), effector memory (EM) and terminally differentiated effector memory T cells (TEMRA) phenotypes in blood (yellow) and lung (blue) from participants with active/ previous TB. (**d**) Frequencies of TNF-α, IL-2, IFN-γ and IL-17 producing CD4^{+} and CD8^{+} T-cells from blood (yellow) and lung (blue) of participants with active/previous TB. Significance calculated by Mann-Whitney test. * denotes p-values which remained significance after stringent Bonferroni correction for multiple comparisons.

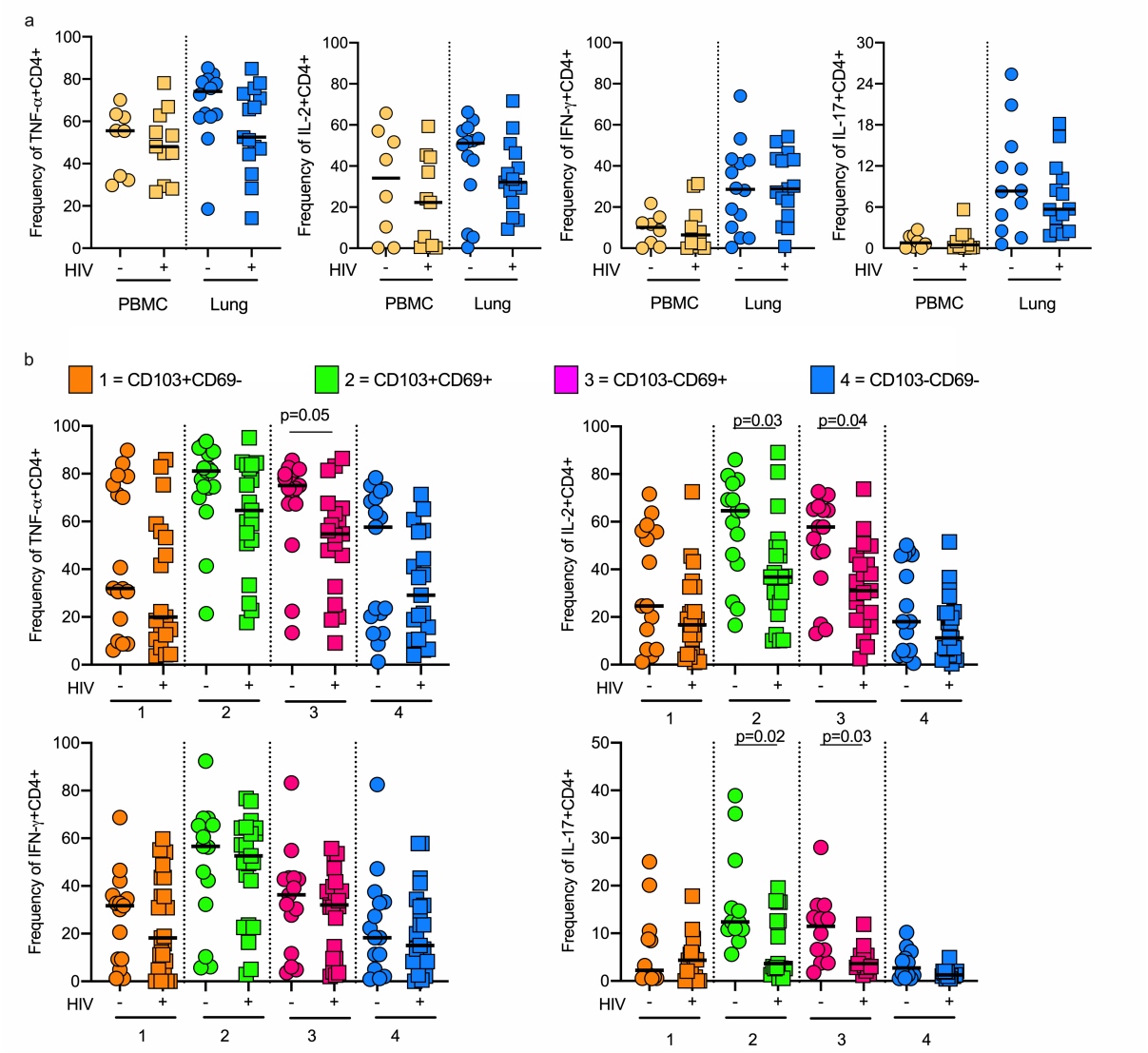

Figure 4. HIV severely depletes cytokine-producing T-cells from the lungs of TB-infected study participants. (**a**) Frequencies of TNF-α, IL-2, IFN-γ and IL-17 producing CD4$^+$T-cells from blood (yellow) and lung (blue) of participants with (squares) and without (circles) HIV co-infection. (**b**) Tissue-resident phenotypes of TNF-α, IL-2, IFN-γ and IL-17 producing CD4$^+$T-cells from lung from participants with (squares) and without (circles) HIV co-infections, where 1 (orange) = CD103$^+$CD69$^-$, 2 (green) = CD103$^-$CD69$^+$, 3 (pink) = CD103$^+$CD69$^+$ and 4 (blue) = CD103$^-$CD69$^-$. Significance calculated by Mann-Whitney test and in all cases median values indicated with a black line.

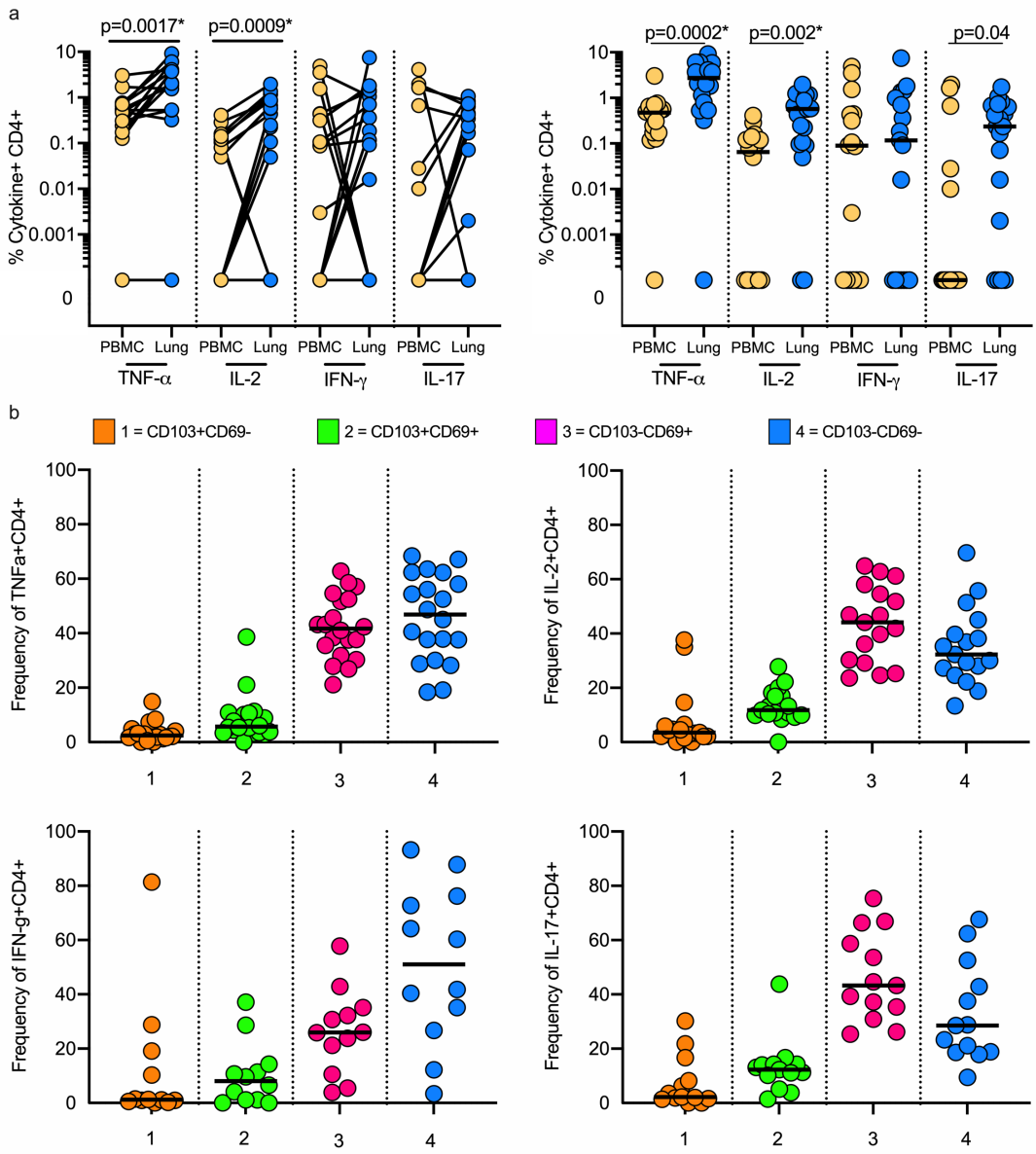

Figure 5. A portion of lung T-cells are TB-specific and produce cytokines in response to *Mtb* peptides. (**a**) Frequencies of TB-specific TNF-α, IL-2, IFN-γ and IL-17 producing $CD4^+$T-cells in paired blood (yellow) and lung (blue) samples from the same participant. Significance by Wilcoxon matched pairs signed rank test. (**b**) Frequencies of TB-specific TNF-α, IL-2, IFN-γ and IL-17 producing $CD4^+$T-cells in blood (yellow) and lung (blue) samples from participants with active/previous TB. Significance by Mann-Whitney test. * denotes p-values which remained significant after stringent Bonferroni correction for multiple comparisons. (**c**) Tissue-resident phenotypes of TNF- α, IL-2, IFN-γ and IL-17 producing $CD4^+$T-cells where 1 (orange) = $CD103^+CD69^-$, 2 (green) = $CD103^-CD69^+$, 3 (pink) = $CD103^+CD69^+$ and 4 (blue) = $CD103^-CD69^-$. Significance calculated by Kruskal-Wallis test, although none was found

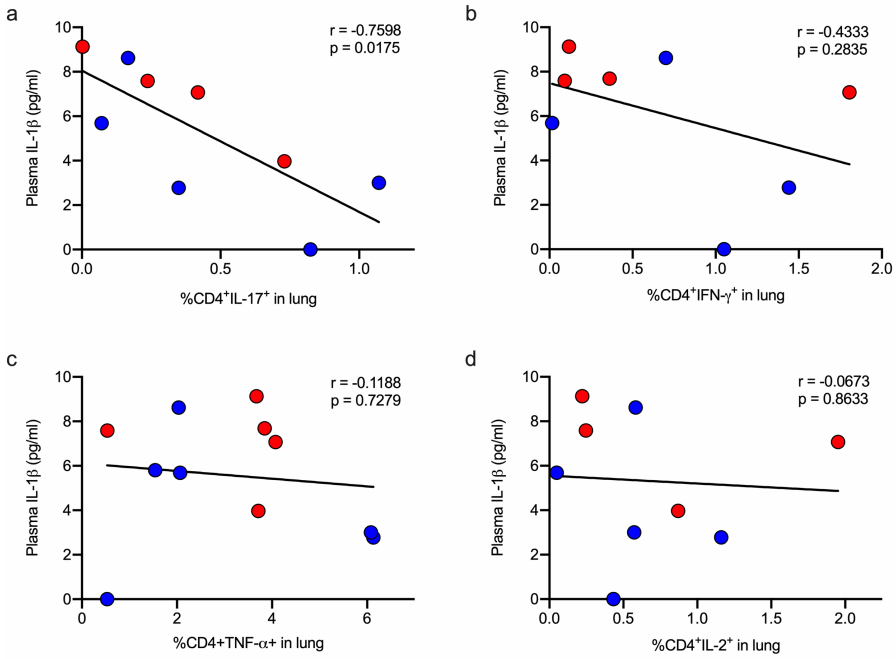

Figure 6. IL-17 producing Mtb-specific CD4 T-cells in lung homogenate inversely correlate with systemic markers of inflammation. Correlations between plasma IL-1 and TNF-α, IL-2, IFN-γ and IL-17 producing CD4+T-cells in lung tissue from participants with active TB (red) or previous TB (dark blue) (**a-d**).

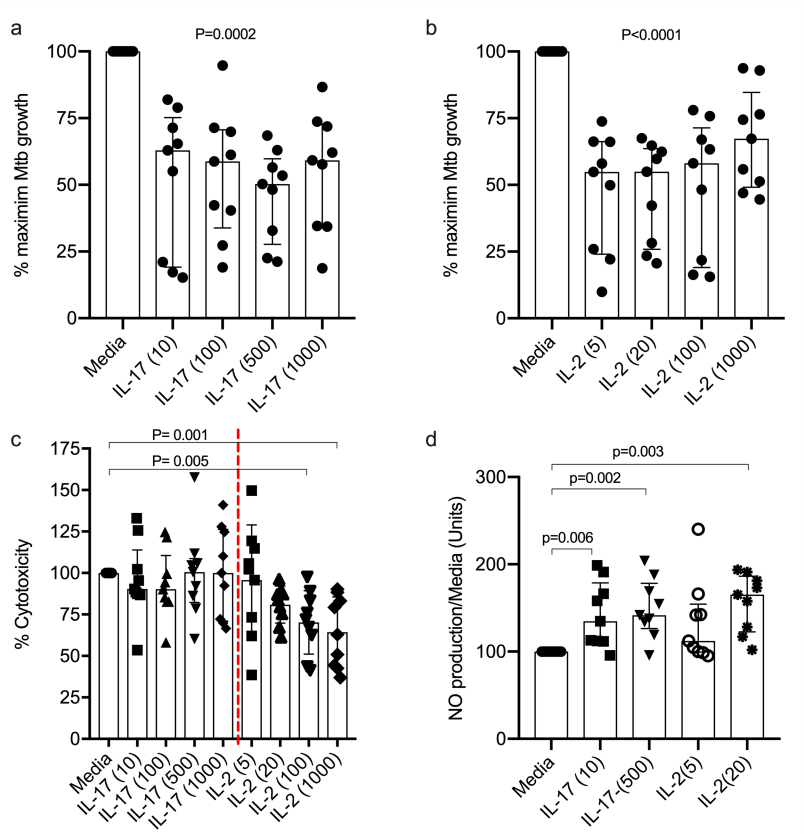

Figure 7. Exogenous IL-17 and IL-2 decreases Mtb growth in 3D-culture system. (a-b). Addition of IL-17 and IL-2 to culture media decreases Mtb growth in granuloma like 3D-human cell culture system. Data from 3 separate experiments using PMBC from 3 different healthy controls conducted in triplicate. Concentrations shown in brackets (ng/ml). Impact of exogenous IL-17 and IL-2 on **(c)** cell viability in above experiments as measured by concentration of lactate dehydrogenase (LDH) in culture supernatant on day 7; and **(d)** production of nitric oxide (NO). Statistical differences for (a-b) tested by Kruskal-Wallis, with Dunn's correction for multiple comparisons (c-d)